

Duality, inverse problems and nonlinear problems in solid mechanics

Modelling of damage induced by contacts between solids

Ky Dang Van

Laboratoire de mécanique des solides, UMR 7649 CNRS, École polytechnique, 91128 Palaiseau cedex, France

Abstract

Prediction of damage induced by contact between solids (rolling–sliding contact or small oscillatory contacts inducing fretting-fatigue) is still a challenge. Complex plastic flows in the contact region lead to difficult calculations in order to derive the stabilized stress and strain states in the regions where damage occurs. For this purpose, three specific computational algorithms are proposed. The fatigue damage prediction methodology, based on a multiscale approach and on the shakedown assumption, is applicable to multiaxial fatigue conditions. This article proposes a short review of the recently developed methods in this area and discusses a series of examples. **To cite this article:** *K. Dang Van, C. R. Mecanique 336 (2008).*

© 2007 Académie des sciences. Published by Elsevier Masson SAS. All rights reserved.

Résumé

Modélisation des endommagements induits par les contacts entre solides. Les endommagements induits par les contacts répétés entre solides (tels ceux dus au roulement–glissement ou aux contacts avec petits débattements qui peuvent entraîner des phénomènes de fretting fatigue) sont particulièrement difficiles à modéliser. Les déformations plastiques générées par ces types de chargement sont complexes à évaluer, notamment pour estimer les états mécaniques asymptotiques dans les zones où les endommagements sont susceptibles de se produire. D'autre part, l'amorçage des fissures de fatigue se produit sous chargements multiaxiaux variables. Afin de surmonter ces difficultés, trois algorithmes spécifiques de calculs élastoplastiques sont tout d'abord proposés. Une approche multiaxiale de la fatigue basée sur une modélisation multiéchelle et sur le concept d'adaptation est ensuite utilisée pour prédire les fissurations observées sur les rails et sur des disques de turbines. **Pour citer cet article :** *K. Dang Van, C. R. Mecanique 336 (2008).*

© 2007 Académie des sciences. Published by Elsevier Masson SAS. All rights reserved.

Keywords: Damage; Multi-axial fatigue; Fretting; Moving loads; Shakedown; Finite element analysis

Mots-clés : Endommagement ; Fatigue multiaxiale ; Fretting ; Adaptation ; Éléments finis

1. Introduction

Contact between solids may induce different types of fatigue defects which are very difficult to model. For instance, the prediction of damage and wear induced by rolling–sliding contact is of primary importance for the railway industry. Therefore, one has to evaluate the mechanical state induced by railway traffic generating complex stress and strain distributions. Moreover, in many cases, the occurrence of damage involves plastic strain, and the determination of

E-mail address: dangvan@lms.polytechnique.fr.

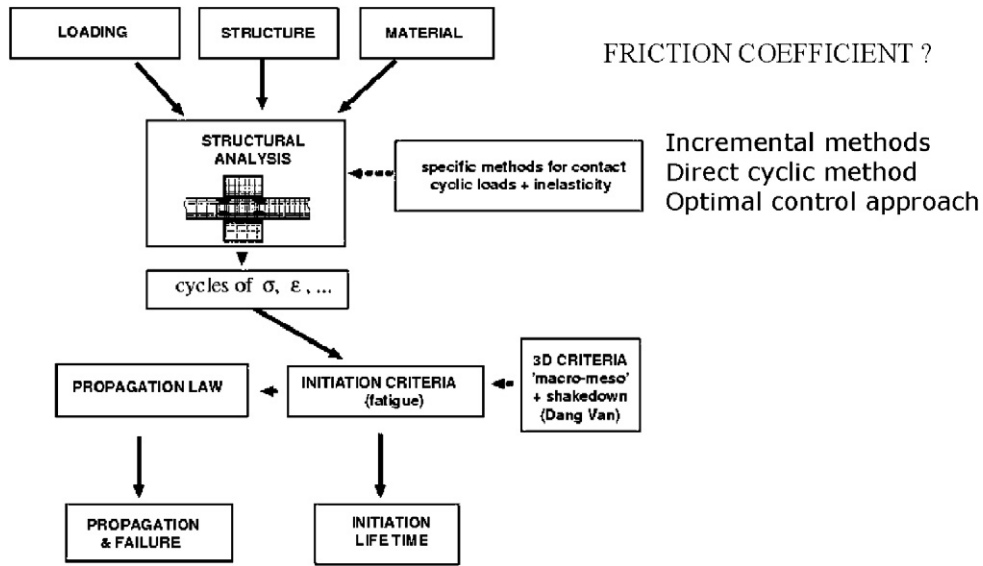


Fig. 1. General methodology for designing structures.

the limit response under repeated loadings requires special computational methods in order to make the calculations tractable within a reasonable time. Finally rolling contact loading generates complex three dimensional varying stress and strain states which cannot be easily reduced to an equivalent stress or strain for the fatigue prediction. As a consequence, fatigue phenomena induced by rolling sliding contact in rails are still difficult to model and no fully satisfactory approaches are yet available.

Another important example of contact damage is the fretting-fatigue defined as a surface damage induced by small amplitude oscillatory displacements between metal components in contact. Depending on the imposed force or the displacement amplitudes, damage is either wear or crack nucleation. In industrial structures, fretting can be at the origin of catastrophic failures which are particularly difficult to predict. In order to study this phenomenon, different authors, [1,2] have established test methodologies using different laboratory experimental set up. The results are generally presented as fretting maps, and are useful for the qualitative understanding of damage formation. They show that fatigue crack initiation occurs in the ‘mixed stick–slip’ regime. Within this regime, relations between the tangential load T , the displacement d and the number of cycles to failure N evolve in a characteristic way: the first loops differ from the stabilised loops in which T and d are proportional. Unfortunately, these parameters are not intrinsic and the obtained results cannot be used for the prediction of fretting on different structures. Another methodology applicable to any kind of structure and loading is needed. For this purpose one must first evaluate the local stress and strain resulting from the cyclic contact loading and second use a multiaxial fatigue criterion in order to predict the crack initiation. For the first task, only numerical calculation is possible. For fretting results from oscillating contact loadings, different elastoplastic computational methods can be used. The incremental method, based on a step by step integration, can be employed to calculate the possible stabilised state, but it imposes cumbersome and lengthy calculations. In order to avoid this drawback some new methods are proposed.

In conclusion, the general methodology proposed here for designing structures (see Fig. 1) which may undergo damage arising from contact between solids is summarized in the scheme represented above. In order to be able to perform the calculations, the local friction coefficient μ , must be known. However, this parameter is generally not precisely determined. For instance, in classical mechanics μ is often taken between 0.1 and 0.3. This range of values for μ is generally used by railway engineers. However, direct measurements developed recently [3] lead to much higher values, sometimes as high as 0.9 or 1. Moreover, this coefficient may depend of the load and the rolling–sliding regime (traction or braking) as it is shown in some studies [4]. Evaluation of the local value of this parameter is still a open question. In the following, we shall just consider different possible values of this parameter in order to discuss the influence of the friction coefficient on the different observed types of contact damage.

2. Evaluation of the stabilised mechanical states due to moving contacts

The prediction of the risk of damage occurrence on a solid submitted to repeated moving contact requires first to evaluate the intrinsic thermo-mechanical parameters and their evolution in the vicinity of the contact zone. As the loading is in general high, plastic flow occurs and the corresponding asymptotic state is either elastic shakedown, plastic shakedown or ratchet. Depending on the load level, the determination of the eventual stabilised state necessitates sometimes thousands of cycles. Therefore, the use of classical incremental methods is not recommended, and we have proposed for these applications other approaches [5].

Stationary methods are efficient for the evaluation of stress and strain in rail: (i) the *pass by pass stationary method* (PPSM) is suitable for studying the build-up cycle by cycle of the plastic strain and the residual stress distributions; (ii) *the direct stationary method* (DSM) permits the direct determination of the stabilised state in the case of shakedown (elastic or plastic), and the characterisation of the ratcheting (non-convergence of the algorithm).

The (iii) *direct cyclic method* is an alternative for studying the same kind of problems as previously mentioned. However, in the case of arbitrary cyclic loadings resulting, for example, from oscillatory contacts, only this last method is applicable.

Another promising method, which will not be discussed in this article, was proposed by M. Peigney and C. Stolz [6]. It is based on optimal control techniques.

3. Recall of the stationary method

This method was already presented in previous papers [5,7]. It applies to a structure (a rail in the presented applications) subjected to contact loads moving with a velocity V in a fixed direction e_z (the longitudinal axis of the rail). Assuming a steady state in a reference frame moving with the loads, the time derivative of any material quantities becomes:

$$\dot{B} = -B, z \quad (1)$$

Writing the equations governing the problem in the moving frame related to the load, one obtains modified balance equations:

$$\operatorname{div} \sigma = \rho V^2 u_{,zz}$$

and constitutive laws:

$$\sigma = L\varepsilon^e + \sigma^0$$

$$A_k = Z : \alpha_k$$

$$\varepsilon = \varepsilon^e + \varepsilon^p$$

$$-\varepsilon_{,z}^p = \Lambda \frac{\partial f}{\partial \sigma}, \quad f(\sigma, A_k) \leq 0, \quad \Lambda \geq 0, \quad \Lambda f(\sigma, A_k) = 0$$

$$\alpha_{k,z} = \Lambda \frac{\partial f}{\partial A_k}$$

where Λ denotes the plastic multiplier, f the yield function, σ^0 the initial stress, α_k are internal parameters and A_k their associated forces linked by the tensor Z , L is the fourth order elastic coefficient tensor.

As described in Eq. (1), time derivatives have been replaced by space derivatives so that the integration of the previous set of equations is performed in space, along the direction of motion of the loads. In this method, neither the load nor the structure have to be translated.

Two numerical procedures for the determination of the stabilised state are derived.

The first one is the *pass by pass stationary method* (PPSM) for the calculation of a single pass. Repeating the procedure for the successive passes, the method computes the stabilised state and its characteristics (number of cycles before reaching the stabilised state, residual stresses, plastic deformations, other internal parameters. . .). The stabilised state can be ratcheting, and in such a case, the ratcheting rate corresponds to surface displacement or plastic strains caused by a pass.

In the second procedure called ‘*Direct stationary method*’ (DSM), the possible stabilised state due to repeated moving load is searched directly. The stress field should be periodic, the plastic strain field and the field of other internal parameters also in the absence of ratcheting. The ratcheting is indicated by a non-convergence of the method.

These methods permit computation of strains and stresses in the rail due to repeated moving contacts.

4. Recall of the ‘Direct cyclic method’

This method proves its efficiency in the case of arbitrary cyclic loading resulting from small oscillatory contacts. The main idea is to take advantage of the periodicity of the loading. The stabilised mechanical response is either a shakedown state or is ratcheting. Knowledge of the exact evolution of the cycles is of limited interest. The *direct cyclic method* (DSM) allows the determination of the asymptotic response of the structure without following the loading step by step.

Let us denote by $F^d(t)$, $t \in [0, T]$, the external loading path of period T corresponding to either fixed or moving contact. The interval $[0, T]$ is discretized in n intervals $0 < t_1 < \dots < t_n = T$. In order to seek directly the asymptotic elastoplasticity solution, we proposed the following iterative procedure. For each internal elastoplastic iteration j at time t_i , we first seek the stress tensor σ_i^{js} which is statically admissible with the loading $F^d(t_i)$ and the strain tensor ε_i^j , which is cinematically admissible with the prescribed displacement $U^d(t_i)$ corresponding to the instant t_i . These two conditions are equivalent to the resolution of equilibrium equations:

$$K U_i^j = Q_i + Q_i^{p^{j-1}}$$

in which Q_i , $Q_i^{p^{j-1}}$, and K represent the nodal external forces corresponding to $F^d(t_i)$ the vector of loads due to plastic strain $\varepsilon_i^{p^{j-1}}$ (assumed known) and the stiffness matrix of the linear elastic structure respectively.

In a second stage, we determine the stress tensor σ_{i+1}^{jp} plastically admissible. For that, at each time, the plastic strain ε_{i+1}^{jp} is obtained by projecting the strain increment $\varepsilon_{i+1}^j - \varepsilon_i^j$ on the elastic convex domain defined by the initial state $(\sigma_i^{jp}, \varepsilon_i^j, \varepsilon_i^{pj})$ at time t_i which is known. σ_{i+1}^{jp} is then calculated from the constitutive law written in incremental form:

$$\varepsilon_{i+1}^j - \varepsilon_i^j = K(\sigma_{i+1}^{jp} - \sigma_i^{jp}) + (\varepsilon_{i+1}^{pj} - \varepsilon_i^{pj})$$

The stabilised state is obtained when the plastic strain ε_1^{pj} at the beginning of the cycle is the same as at the end of the cycle ε_n^{pj} . Otherwise, the same steps are performed in the iteration $j + 1$ by initialising $\varepsilon_1^{p^{j+1}}$, $\varepsilon_n^{p^{j+1}}$ to ε_n^{pj} , ε_1^{pj} and the process is repeated until elastic or plastic shakedown is achieved. Ratcheting is revealed by the non-convergence of the procedure.

Comparison between this method and incremental method presented in [8], proves the validity and the efficiency of the DCM method.

5. Fatigue treatment

Prediction of damages induced by moving contact loadings (rolling contact, or structures undergoing fretting ...) necessitates the use of multi-axial fatigue criteria able to deal with complex multi-axial situations. In fact, the local stress and strain fields are completely tri-dimensional with no fixed directions during their evolution. It is important to describe in a fatigue criterion the main features of the loading paths at any point of the structure. For this purpose a unified fatigue approach was proposed based on multi-scale approach and shakedown assumption. This new point of view on the fatigue strength and the fatigue damage gives a general framework to fatigue modelling, for high cycle as well as for low cycle. It allows analyzing, in an efficient manner, all types of industrial fatigue problems, including contact.

It is well known that the fatigue phenomenon in metals is associated with the movement of dislocations and creation of persistent slip bands in metal grains. Conducting classical laboratory tests the following features can be observed: in the high cycle fatigue (HCF) regime, the stress amplitude is low, the test specimen remains globally elastic and plasticity is localized in some well oriented grains; in the low cycle fatigue (LCF) regime, plasticity occurs at the

structural level as well as the grain level. However, the fatigue mechanisms are the same in both cases and the different fatigue regimes differ essentially in the spatial extension of the plasticity. In order to propose a unified view for fatigue modelling, we shall suppose that the fatigue initiation corresponds to the limit of shakedown possibility of the material in both scales. In what follows we shall distinguish the mesoscopic scale corresponding to the grain and the macroscopic scale used by engineers which supposes implicitly the concept of representative volume element (RVE) defines as sufficiently small volume so that one can distinguish the microscopic heterogeneities and sufficiently large to be representative of the macroscopic behavior. σ' , ϵ' , ϵ'_p , ρ' are respectively the stress strain, plastic strain and residual stress tensors at the mesoscopic scale, and σ , ϵ , ϵ_p , ρ are the corresponding macroscopic quantities. Engineers calculate the mechanical parameters of a structure not at a point but over a volume that defines the scale which is used. In this volume centered on that point, stress and strain σ and ϵ are assumed constant. However, this volume contains grains which are heterogeneous. In HCF, at the mesoscopic level, plasticity occurs in certain number of grains and generates heterogeneous plastic strain and local residual stress states distribution in the RVE. Since the first cracks initiate in these positions, $\sigma'(t)$ should be evaluated here. This problem corresponds to a localisation problem which cannot be solved without some additional assumptions.

The relation valid at any time t of the loading between macroscopic and mesoscopic stresses is:

$$\sigma' = \mathbf{L} \cdot \sigma + \rho'$$

where \mathbf{L} is the elastic localisation tensor and ρ' is the local residual stress tensor linearly related to plastic strains. The additive term thus depends of the loading path. In order to calculate σ' , we suppose that shakedown occurs before fatigue. More precisely, we assume that fatigue corresponds to the limit elastic shakedown possibility of the structure at the mesoscopic and macroscopic scale.

Thank to this assumption, one can apply theoretical results such as the Melan–Koiter static shakedown theorem or its extension to *generalised standard materials*; see Q.S. Nguyen [9]. (We recall that generalised standard materials are suited for description of material behaviour of metals.) This last result, which gives a sufficient condition for elastic shakedown, can be stated as follows:

“If there exist a time θ and a fixed generalized self equilibrated stress field $[\rho(x), \mathbf{A}(x)]$ and a safety coefficient $m > 1$ such that for any point x of the structure and $\forall t > \theta$, $f[m(\sigma_{el}(x, t) + \rho(x)), m\mathbf{A}(x)] < 0$, the structure will shakedown elastically.”

$f(\sigma, \mathbf{A})$ represents the material yield function, \mathbf{A} correspond to ‘forces’ associated to hardening parameters. Thus, $(\rho(x), \mathbf{A}(x))$ are generalized ‘residual stresses’. σ_{el} is the stress response of the structure under the same external loading, but under the assumption that the constitutive material has a pure elastic behavior.

This theorem is however difficult to apply, since, the residual stress field ρ must be self equilibrated, a condition which is difficult to fulfill. Another proposal due to Mandel et al. [10] opens a possibility to overcome this difficulty; the plasticity criterion can be written $J_2[(\sigma - \alpha)] < k^2(P_{eq})$; α the kinematic strain hardening parameter is the center and k (P_{eq}) the isotropic parameter is the radius of the actual convex of plasticity. Generally, k increases with equivalent plastic strain P_{eq} until some maximum value k^* and then decreases. Since $\sigma = \sigma_{el} + \rho$, one obtains:

$$J_2[(\sigma_{el} - \mathbf{z})] < k^2(P_{eq})$$

where $\mathbf{z} = \alpha - \rho$. \mathbf{z} is not necessarily self-equilibrated since α has not to fulfill this condition.

For cyclic loadings, σ_{el} and ρ are functions of time t ; however, $\mathbf{z}(t)$ must be inside or on the convex (hypersphere) with center $\sigma_{el}(t)$. The trajectory of $\sigma_{el}(t)$ is known at any point x of the structure because it is the solution of an elastic problem.

Shakedown may occur only if for $t > \theta$ the intersection of these convex is not empty. The limit case of possible elastic shakedown occurs when the intersection domain is reduced to a point, for a value corresponding to the maximum of $k^2(P_{eq}) = k^$. The dissipated energy density required for reaching this limit state corresponds to the local bound for possible shakedown. Beyond this bound failure will occur.*

We use these different results at different scales in order to propose fatigue modeling. We shall make the following fundamental assumption: *fatigue corresponds to the limit of elastic shakedown possibility of the material of the structure at the mesoscopic and macroscopic scale.* We then examine the consequences of this hypothesis in order to derive a unified fatigue modeling and the associate computational methods for high cycle and low cycle fatigue.

5.1. High cycle fatigue

Characteristics of this fatigue regime are: (i) the loadings are not very important, (ii) the structure is globally elastic; and (iii) fatigue failure initiates only in some grains. It is difficult to evaluate directly the plastic strains and the dissipated energy in the grains that will fail. It is more judicious to proceed indirectly by an inverse way: since the fatigue limit corresponds to the shakedown limit, one can evaluate the local stress at the stabilized state if these grains are at or near the fatigue limit. Starting from the knowledge of $\sigma(x, t)$ at a point x of the structure, we derive the local stress σ' by constructing the smallest hypersphere containing $\sigma(x, t)$ the center of which corresponds to $\sigma^* = \alpha^* - \rho^* \approx -\rho^*$, because it can be shown that $|\alpha^*|/|\rho^*| \ll 1$.

Thus we have an estimation of the local stress tensor $\sigma'(t) = \sigma(t) + \rho^*$ in grains which may fail by fatigue. Different fatigue criteria can be formulated based on the stabilized stress tensor:

- for instance a linear combination of shear τ and concomitant hydrostatic tension p (Dang Van criterion):

$$\tau + ap < b$$

- Papadopoulos criterion:

$$k^* + ap_{\max} < b$$

can be interpreted in the same way: the radius of the elastic domain at the limit state of possible shakedown depends of the maximum hydrostatic tension in the loading cycle.

The different computational steps for the application of these criteria can be found, for instance, in Ref. [11].

5.2. Low cycle fatigue

In this regime macroscopic plastic strain is important and then difference between ε_p and ε_p' decreases so that there is few difference between macroscopic and mesoscopic parameters. However we propose to choose the dissipated energy W because it is a scalar parameter easy to compute (particularly in presence of thermo-mechanical loadings) and which leads to good predictions on structures. The fatigue criterion can be simply expressed by a relationship, where N is the number of cycles required for crack initiation:

$$W = cN^b$$

In order to improve the predictivity of the previous relation when high triaxiality is present, it is possible to introduce the hydrostatic pressure in the criterion:

$$(W + ap_{\max}) = cN^b$$

6. Application to analysis of some rail damage

Different types of fatigue cracks may appear in the rail head, in the vicinity of the rolling track. These defects are of different natures. In the French railways they depend on the time period. From the 1960s to the early 1970s, the 'kidney shape cracks' are the most frequently encountered. They initiate in the rail head quite far from the rolling surface (around 7 mm) and propagate downwards in the rolling direction. Nowadays, squats and head checks are encountered on straight tracks or shallow curves. Contrary to the kidney shape cracks they initiate very near from the surface (some hundreds of microns to mm) on quite a long distance in the deformed zones of the running track. When they reach a certain size below the surface, they can propagate downwards to form progressively transverse cracks which propagate quite fast. That is the reason why their prevention is necessary. Head checks are angle cracks similar to squats which appear on the high rail in curves and crossing rails. The reasons of this difference between the two types of observed damage (in the depth and near the surface) are, on the one hand the nature of the rail steel (in the 1960s, the rail heads contained many inclusions due to the use of the Thomas process steels) and, on the other hand, the increasing of load and power per axle. The snake skin defect is typically found in some parts of the RER network (Réseau Express Régional) of Paris. It occurs near some railway stations with very high density and heavy

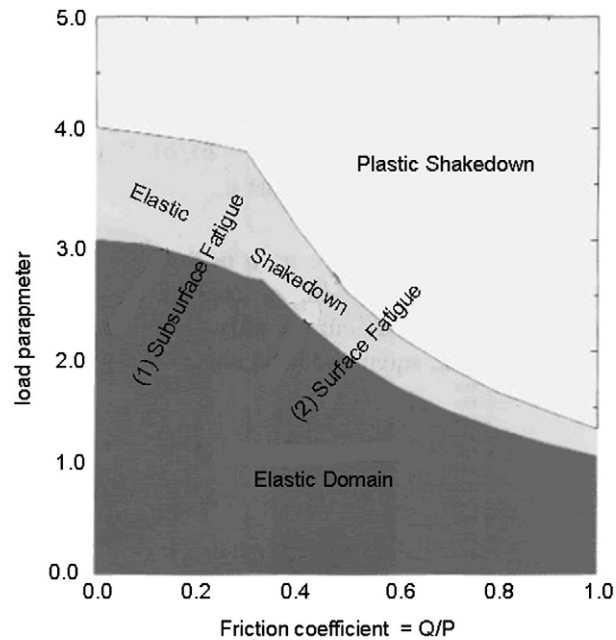


Fig. 2. Numerical shakedown and fatigue map for line contact and full sliding.

traffic in the acceleration and deceleration region of the rails. These defects correspond to surface micro-crackings, approximatively parallel to the rolling–sliding direction.

To understand the circumstance of occurrence of these defects, studies were undertaken using the proposed methodology:

- First we compute strains and stresses in the rail due to repeated moving contacts, using the stationary algorithms presented previously, in order to determine the nature of the stabilised state in relation to the traffic and the type of rail steel (elastic shakedown, plastic shakedown or ratcheting).
- Then we use the multiaxial high cycle fatigue criterion to predict the fatigue behaviour of rails.

6.1. Kidney shape cracking

The 2-D calculations were performed to evaluate the stabilized state and the residual stress pattern in the rail symmetry surface at different depths. In this way, we obtained the local stress cycle for different traffic conditions. Application of the fatigue criterion allows us to predict the locus of the crack initiation in relation with the load parameters. For instance, in the case of a 2D Hertzian contact and full sliding, the results obtained are summarized on Fig. 2. This type of fatigue corresponds to the region 1 of the map: initiation in depth, high cycle fatigue in the elastic and elastic shakedown zones.

Region 2 where friction coefficient becomes important corresponds to surface damage.

The method we propose is applicable for any kind of rolling, with and without sliding regime.

6.2. Analysis of squat and head check

A complete 3-D rolling contact simulation was performed to simulate the phenomena. In this case, the microscopic observations of the orientations of the fibers in the running zone show that the superficial contact effects have to be taken into account. In these observations one can distinguish different fibers orientations (corresponding to severe local superficial plastic flow) depending on the position on the rail head surface and squat damage appears in a precise place. Dynamic contact on wheel–rail system calculations performed by INRETS, based on Kalker method, shows complex evolution of the rail–wheel contact with different shapes of the contact area, pressure and spin distribution. To simulate the phenomena, we choose to reproduce a simplified sequence, consistent with the real cinematic. The PPSM

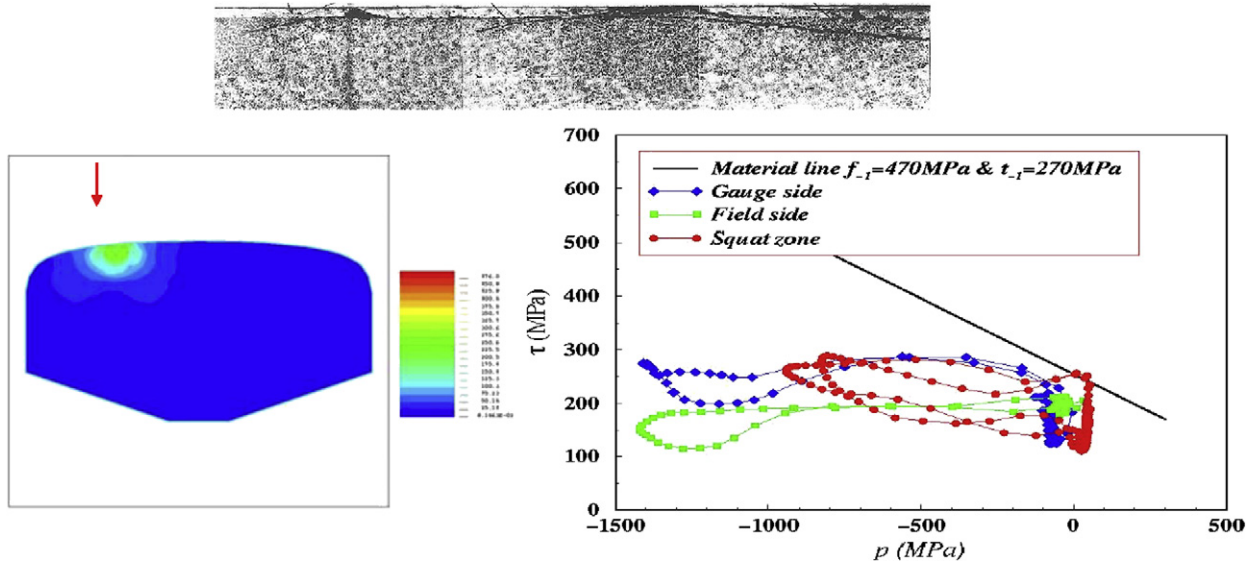


Fig. 3. Squat modelling: loading path at gauge side, field side and central zone where crack initiates.

method was used to make calculations for the evaluation of the mechanical state in the rail. Finally, fatigue analysis was conducted using the multiaxial fatigue criterion, thanks to a specific analysis software. The constants a and b of the criterion are determined using fatigue limit of the rail steel determined by classical fatigue tests (rotating-bending $f_{-1} = 450$ MPa, alternate torsion $t_{-1} = 270$ MPa). The stresses are calculated at the stabilized state reached after the contact sequence mentioned previously. On Fig. 3 the loading path of three different points (gauge side, central zone, field side) of the running surface is shown. It can be seen that the fatigue crack are likely to occur in the central zone.

6.3. Snake-skin defects

The same type of approach was employed. First, the use of the previous dynamic rail–wheel software gives the conditions of contact, then we perform the repeated elastoplastic calculations to determine the stabilized mechanical state, and finally we apply the fatigue multiaxial criterion. The obtained predictions are shown on Fig. 4. We can see that the high friction coefficient increases the danger of snake-skin defect occurrence.

7. Application to fretting fatigue

Our objective is to propose an *intrinsic methodology* to predict fretting which can be applied to any kind of structure. For this purpose, the approach is based on numerical calculations in order to compute the mechanical quantities resulting from the cyclic contact loading. The obtained stabilized stress variation is then introduced in the multiaxial fatigue criterion to check if crack may appear. The first verification of the validity of the proposed method consists in the interpretation the results of a laboratory fretting test.

The following experimental set-up was used by C. Petiot in order to study this phenomenon [12]: it consists of two cylindrical pads clamped by a clamping force P again the two sides of a flat uniaxial fatigue specimen tested in repeated tension under constant amplitude loading $(0, S_{\max})$. The prescribed oscillatory displacement between the pads is linked to the prescribed oscillatory fatigue stress $S(t)$ in the specimen. A special device permits one to measure simultaneously the clamping force and the tangential force $T(t)$ due to friction and related to the accommodation displacements. The variations of $T(t)$ are recorded for each fatigue cycle and plotted as function of the fretting fatigue stress $S(t)$ (called hereafter fretting-fatigue loop). Due to the contact of the pads, the fatigue limit of the specimen decreases in an important manner compared to the fatigue limit without these two pads. In fact, by varying the operating parameters (P, S_{\max}) , three regimes are observed:

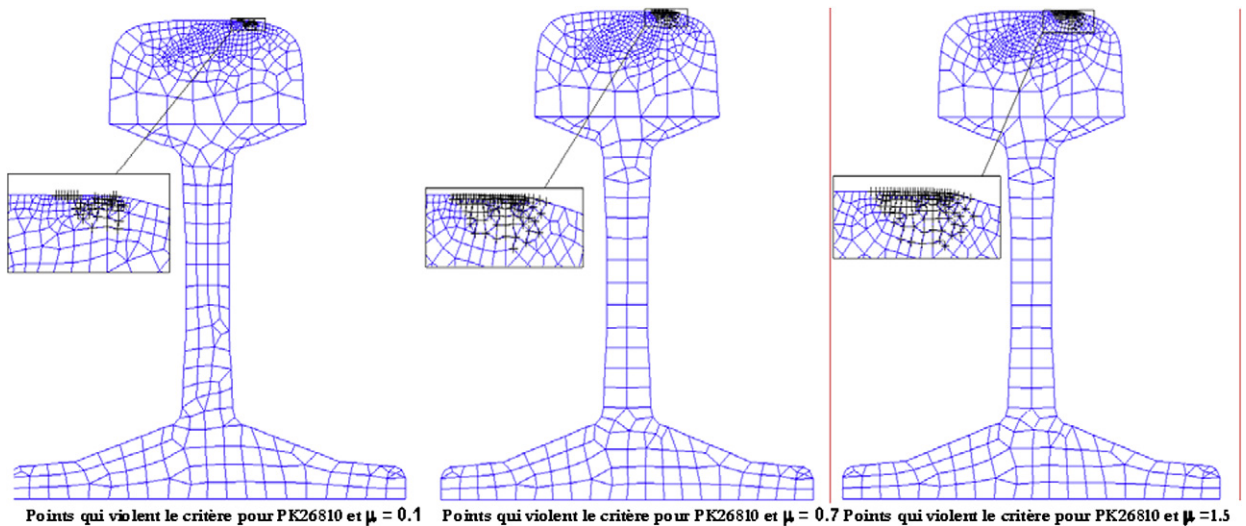


Fig. 4. Danger of ‘snake skin’ occurrence for 3 values of friction coefficients 0.1, 0.7, 1.5.

- *the stick regime*: fretting-fatigue loops are quite linear during the test which means that the displacement between the contacting surfaces is mainly accommodated by elastic deformation. No damage appears during the 10^7 cycles of the test;
- *the mixed stick-slip regime*: The loops start with an closed elliptical shape and stabilized linearly in the same way as in the previous regime. There is partial slip which decreases with the number of cycles. In this regime crack nucleation is observed at the edges of the contact;
- *the gross slip regime*: the loops present a trapezoidal shape corresponding to full slip; in this regime particle detachment is observed corresponding to severe wear.

The question is the following: is it possible to predict the initiation (and no initiation) of cracks in relation with the loading parameters (P , S_{\max} , R , radius of the pads, ...) and the intrinsic material fatigue properties (material Wöhler curve) determined by classical fatigue tests without contact?

In order to calculate the asymptotic stress state near the contacts, C. Petiot et al. [12] used the incremental method, whereas N. Maouche et al. [13] employed the direct cyclic method which is more convenient to use. These stress cycles are then introduced in the Dang Van multiaxial fatigue criterion in order to check the danger of fatigue. The most critical points are located at the surface at the edge of the contact. The most critical loading path (τ , p) for each regime resulting from the stress cycles in the stabilized state is plotted in the (τ , p) diagram shown on Fig. 5. In the sticking regime, the loading path (τ , p) is beneath the fatigue material line, so no damage occurs. In the stick-slip regime, the loading path intersects the material fatigue line, concluding with crack failure. The prediction of crack initiation is thus in good agreement with the experimental observations.

7.1. Prediction of fretting on a turbine disk [14]

Aero-engines incorporate a large number of mechanical joints where fretting-fatigue is an important life-controlling factor. Safety requirements of aeronautic components make prediction and avoidance of fretting-fatigue a critical reliability issue. Blade disk attachments are typical examples. They have to endure high centrifugal forces leading to elevated contact and bulk stress, combined with small relative displacements due to vibrations in operation, make an important, if not the main, design criterion. In order to explore a life method to predict and quantify an industrial fretting fatigue case, engineers of MTU aero engines company studied with the help of researchers from the École polytechnique the turbine spin-pit test performed on a turbine disk configuration [14]. The disk is fitted with 47 blade ‘dummies’ that are connected to the disk by a fir tree-type attachment geometry. A two dimensional plane strain computational model was employed to derive the stress and the strain fields in the contact zone of the disk and the dummy. The calculations were made by incremental methods for ten loading cycles to converge to a stable shakedown

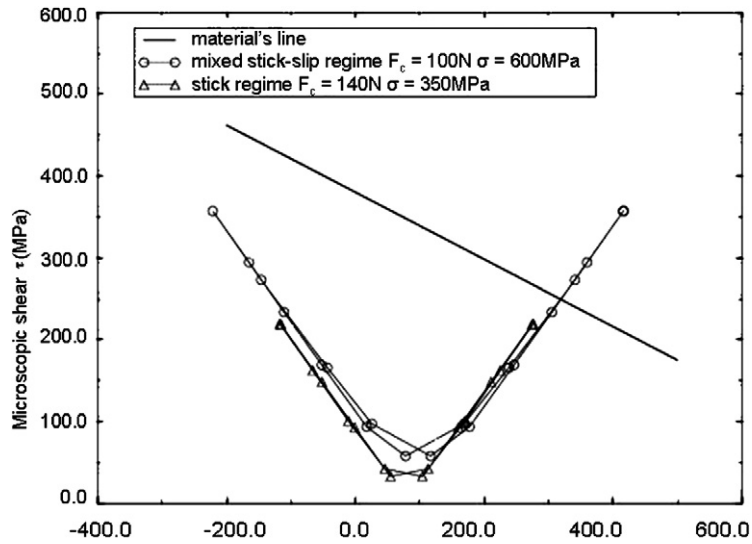


Fig. 5. Loading path in Dang Van’s diagram in stick regime (no crack initiation) and mixed-stick regime (crack initiation because the loading path cross the fatigue criterion).

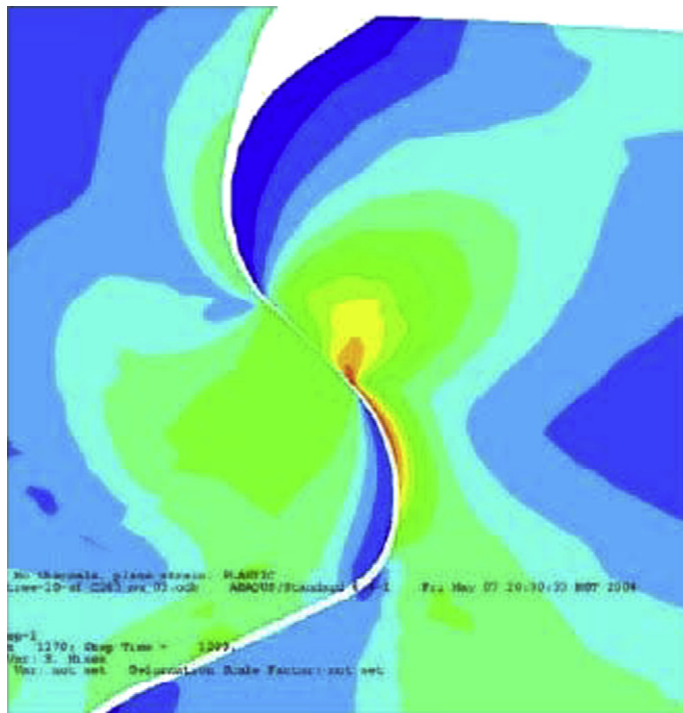


Fig. 6. Distribution of equivalent stress near the contact of turbine-disk configuration at the 10th loading cycle for $\mu = 0.3$.

state. To evaluate the effect of friction coefficient on the fretting fatigue life, several computations were performed with varying friction coefficient μ varying from 0 to 0.9.

Fig. 6 shows the stress distribution on the outer contact lobe of the attachment during the 10th loading cycle for a friction coefficient of 0.3. The highest stress occurs on the trailing edge of the contact on the disk side. Fig. 7 shows the Dang Van loading paths on the critical disk locations for μ of 0, 0.3, 0.9 at one of the critical locations (inner disk lobe). From the lobe, it is clear that for no friction no crack initiation is expected, as the loading path does not cross the material line at any instant during the loading cycle. On the contrary, for higher friction coefficients ($\mu = 0.3, 0.9$),

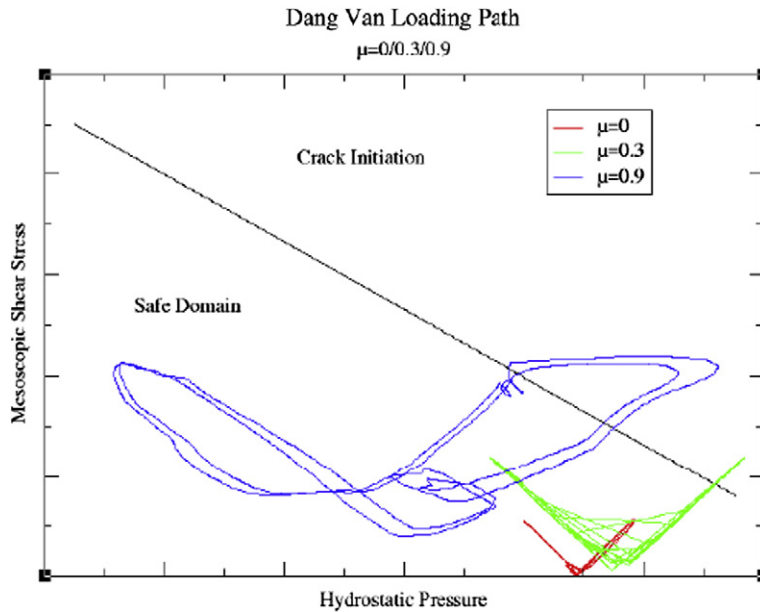


Fig. 7. Loading path in Dang Van diagram for critical locations on the disk surface for $\mu = 0$ (no crack initiation), $\mu = 0.3, 0.9$ (crack initiation).

the loading path crosses the fatigue line during the loading phase. The corresponding critical locations determined by the fatigue criterion lie on the trailing edges on the disk surface. This result matches very well with experimental observations.

References

- [1] O. Vingsbo, S. Söderberg, On fretting maps, *Wear* 126 (1988) 131–147.
- [2] L. Vincent, Y. Berthier, M. Godet, Testing methods in fretting fatigue: a critical appraisal, standardization of fretting fatigue test methods and equipment, in: M. Helmi Attia, R.B. Waterhouse (Eds.), *ASTM STP 1159*, American Society for Testing and Materials, Philadelphia, PA, 1992, pp. 33–48.
- [3] S. Fouvry, P. Kapsa, L. Vincent, A multiaxial fatigue analysis of fretting contact taking into account the size effects, in: *Fretting-Fatigue Current Technology and Practices*, ASTM STP 367, 2000.
- [4] J. Mandel, Résistance au roulement d'un cylindre indéformable sur un massif parfaitement plastique, in: *Le Frottement & l'Usure*, p. 25, Paris; GAMI, [296, 297, 301], 1967.
- [5] K. Dang Van, H. Maitournam, Steady-state flow in classical elastoplasticity: application to repeated rolling and sliding contact, *J. Mech. Phys. Solids* 41 (11) (1993) 1691–1710.
- [6] M. Peigney, C. Stolz, An optimal control approach of inelastic structures under cyclic loading, *J. Mech. Phys. Solids* 51 (2003) 575–605.
- [7] K. Dang Van, H. Maitournam, On some recent trends in modelling of contact fatigue and wear in rail, *Wear* 253 (2002) 219–227.
- [8] N. Maouche, M.H. Maitournam, K. Dang Van, On a new method of evaluation of the inelastic state due to moving contacts, *Wear* 203–204 (1997) 139–147.
- [9] Q.S. Nguyen, *Stabilité et mécanique non linéaire*, Hermes, 2000.
- [10] J. Mandel, B. Halphen, J. Zarka, Adaptation d'une structure élastoplastique à écoulement cinématique, *Mech. Res. Comm.* 4 (1977) 309–314.
- [11] K. Dang Van, Fatigue analysis by the multiscale approach, in: *High Cycle Metal Fatigue, From Theory to Applications*, in: K. Dang Van, I.V. Papadopoulos (Eds.), C.I.S.M. Courses and Lectures, vol. 392, Springer, 1999.
- [12] C. Petiot, L. Vincent, K. Dang Van, N. Maouche, J. Foulquier, B. Journet, An analysis of fretting-fatigue failure combined with numerical calculations to predict crack nucleation, *Wear* 181–183 (1995) 101–111.
- [13] N. Maouche, M.H. Maitournam, K. Dang Van, On a new method of evaluation of the inelastic state due to moving contacts, *Wear* 203–204 (1997) 139–147.
- [14] H.V. Arrieta, P. Wackers, K. Dang Van, A. Constantinescu, H.M. Maitournam, Modelling attempts to predict fretting-fatigue life on turbine components, in: *RTO-AVT Specialists Meeting on "The Control and Wear in Military Platforms"*, Williamsburg, USA, June 2003, published in RTO-MP-AVT-109.